

## Short communication

## Effect of fly ash cenospheres on the microstructure and properties of silica-based composites

Caifen Wang, Jiachen Liu<sup>\*</sup>, Haiyan Du, Anran Guo*Key Lab of Advanced Ceramics and Machining Technology of Ministry of Education, School of Materials Science & Engineering, Tianjin University, Tianjin 300072, China*

Received 19 August 2011; received in revised form 15 January 2012; accepted 16 January 2012

Available online 25 January 2012

**Abstract**

Effects of fly ash cenospheres on the microstructure and properties of silica-based composites were studied in this paper. It was found that the density of the samples decreased as the content of fly ash cenospheres increased, while the strength increased inversely when the content was lower than 50 wt%. An interlaced microstructure of lath-like and needle-like mullite crystals was discovered in the composites, which was a beneficial factor for strengthening the silica matrix. Furthermore, the results indicated that fly ash cenospheres can promote the densification of silica as a sintering aid and restrain the crystallization of cristobalite as an inhibitor. After sintered at 1200 °C for 2 h, the density and flexural strength of silica-based composites with 50 wt% fly ash cenospheres were 0.92 g/cm<sup>3</sup> and 14.5 MPa separately, and the strength was as high as that of the silica ceramics without fly ash cenospheres.

© 2012 Elsevier Ltd and Techna Group S.r.l. All rights reserved.

**Keywords:** B. Composite; B. Porosity; C. Mechanical properties; Silica; Microstructure**1. Introduction**

Nowadays, the recycling of industrial waste to produce highly valuable materials attracts great attention. Fly ash cenospheres are the hollow particles in fly ash formed by the rapid cooling of glass during the combustion process of coal [1]. Fly ash is the by-product generated from coal-fired power plants and it has caused serious environmental pollution. In the past decades, people have tried a lot to utilize this kind of waste to reduce the pollution and to produce high value products. Due to their hollow nature, fly ash cenospheres always present low density (0.4–0.8 g/cm<sup>3</sup>) and good insulation, and as a result, they have received much attention as raw materials for the fabrication of light weight composites [2]. In recent years, a great deal of research has focused on utilizing fly ash cenospheres (FACs) to prepare porous light weight composites. The cements have been mixed with cenospheres in order to reduce the density and improve the thermal insulation [3,4]. The FAC was also used as a filler and reinforcement in metal-matrix composites (MMCs) [5,6] and

polymer-matrix composites (PMCs) [7–9]. However, the low-density ceramic-matrix composites with FACs are rarely reported so far.

Silica ceramics have attracted great research attention due to their low density, low thermal conductivity and excellent thermal-shock resistance. However, the silica ceramics are difficult to be sintered because the sintering temperature is limited by the formation of cristobalite. Cristobalite, one phase of silica, is produced at high temperature and the displacive phase transition of cristobalite possibly takes place at low temperature. During the displacive phase transition, a lot of micro-cracks would appear, so the silica ceramics always present low strength [10].

In this paper, silica composite ceramics with fly ash cenospheres were fabricated in order to reduce the sintered density and enhance the strength. During the heating treatment, FACs melted and diffused into silica to combine with each other, and the closed pores were left in the matrix, inducing the light weight of composite ceramics. Besides, FACs were mainly composed of SiO<sub>2</sub> and Al<sub>2</sub>O<sub>3</sub>, which could form mullite crystals presenting excellent creep resistance and high strength at high temperature. In this way, the strength of silica based composite ceramics was improved. A schematic view was shown in Fig. 1.

<sup>\*</sup> Corresponding author. Tel.: +86 139 02072240; fax: +86 022 27402102.

E-mail addresses: [caifen2008@yahoo.com.cn](mailto:caifen2008@yahoo.com.cn) (C. Wang), [jcliu@tju.edu.cn](mailto:jcliu@tju.edu.cn) (J. Liu).

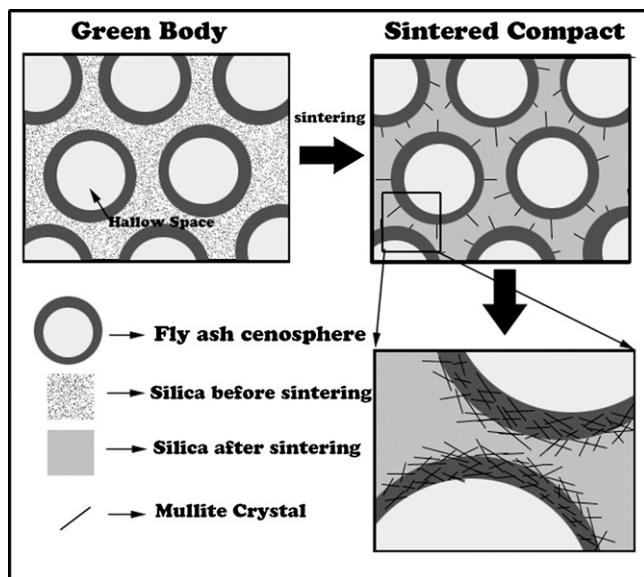


Fig. 1. A schematic view of silica-based composite using fly ash cenosphere as density-decreasing agent and high strength framework.

## 2. Experiment

### 2.1. Materials processing

FACs, obtained from China Coal Group, Shuozhou, Shanxi Province, were rinsed three times with distilled water, and then dried at 110 °C for 24 h. Finally, the uniform spheres were obtained by sieving them through 100 mesh and again 150 mesh. Spheres were mainly composed of mullite, quartz and glass phase, as shown in Fig. 2 and Table 1. The density of obtained sphere was about 0.7 g/cm<sup>3</sup>.

Silica slurry was prepared by ball-milling fused silica powders (>99.9%, Jangsu Hongda Quartz Material Limited Company) with premix solution by the weight ratio of 100:35, and acrylic amides were used as the dispersant. Premix solution were composed of acrylamide (C<sub>2</sub>H<sub>3</sub>CONH<sub>2</sub>), N,N-methyle-nebisacrylamide (C<sub>7</sub>H<sub>10</sub>N<sub>2</sub>O<sub>2</sub>) and distilled water by the weight ratio of 20:2:100.

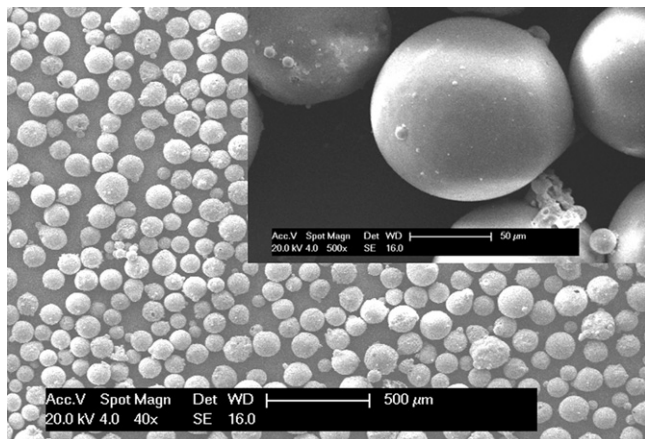


Fig. 2. SEM of fly ash cenospheres.

Table 1

Typical chemical composition of FAC in weight percent.

Chemical composition of the FAC	Weight percent (%)
SiO <sub>2</sub>	61.9
Al <sub>2</sub> O <sub>3</sub>	28.6
Fe <sub>2</sub> O <sub>3</sub>	4.3
TiO <sub>2</sub>	1.1
CaO	0.8
K <sub>2</sub> O	1.3
Others	2

Spheres were added into the silica slurry by the weight ratio of 0% (S0), 10% (S1), 20% (S2), 30% (S3), 40% (S4) and 50% (S5) and mechanically stirred for 30 min. Ammonium persulfate ((NH<sub>4</sub>)<sub>2</sub>S<sub>2</sub>O<sub>4</sub>) was added as an initiator. Then the slurry was moulded. The mould was heated up to 80 °C for 15–30 min in the drying oven and the gelation process was finished. After gelation, the green bodies were demoulded and dried slowly until the weight remained unchanged. The dried green bodies were then sintered in an electric furnace at 1100, 1200 and 1300 °C, severally. The heating speed and dwelling time were 5 °C/min and 2 h.

### 2.2. Materials characterization

The density and open porosity of the sintered specimens were measured by a conventional method using Archimedes' principle in distilled water medium. The open pores were defined as the interconnected pores that were open to the surface and allowed the penetration of water into specimens. The specific surface area (SSA) values of samples were analyzed by the N<sub>2</sub> adsorption measurement (BET, NOVA-3200e). Room temperature flexural strength was determined by the three-point bending method in a universal materials testing machine (XWW, Beijing Shengxin detecting instrument Ltd., China). Three-point bending strength was measured using bar samples 24 mm × 4.8 mm × 3.6 mm with a span length of 20 mm and a crosshead speed of 0.5 mm/min. All the results were given as the mean values of five measurements. The sintered samples were identified by X-ray diffraction (Cu Ka radiation, D/Max-2500 Rigaku, Japan) and their microstructures were observed by means of scanning electron microscopy (XL30, Philips, Netherlands).

## 3. Results and discussions

### 3.1. Effect of FAC content on density

The density of samples sintered at different temperatures was shown in Fig. 3. As can be seen from Fig. 3, the density increased as the sintering temperature raised from 1100 °C to 1300 °C, which resulted from the densification of silica. On the other hand, the density decreased with the increase of FACs after sintering at the same temperature because of the increasing pores in the matrix. As shown in Table 2, the total porosity increased with the increase of FACs content and the

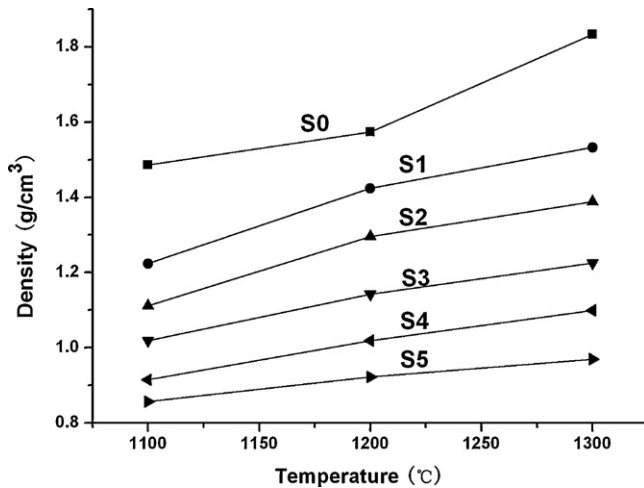


Fig. 3. Density of samples sintered at different temperatures.

increasing in BET surface area values was in agreement with porosity.

Table 2 shows the density and porosity of silica/FACs composites sintered at 1200 °C. The theoretical density of a composite could be calculated using a rule of mixtures as

$$\rho_{th} = \rho_{cw}V_{cw} + \rho_{fs}V_{fs} \quad (1)$$

where  $\rho_{th}$  was the theoretical density of the composite,  $\rho_{cw}$  was the theoretical density of the cenospheres wall (assumed to be 2.9 g/cm<sup>3</sup> [11]),  $\rho_{fs}$  was the theoretical density of fused silica (assumed to be 2.2 g/cm<sup>3</sup>).  $V_{cw}$  and  $V_{fs}$  were the volume fractions of cenosphere wall and fused silica respectively, and volume fraction  $V_i$  could be calculated by Eq. (2), where  $m_{cw}$  represented the mass of cenospheres, and  $m_{fs}$  was the mass of fused silica.

$$V_i = \frac{m_i/\rho_i}{m_{cw}/\rho_{cw} + m_{fs}/\rho_{fs}} \quad (2)$$

The theoretical density of the silica/FACs composite was finally calculated by Eq. (3), where  $w_{cw}$  represented weight percent of FACs, and  $w_{fs}$  was weight percent of fused silica.

$$\rho_{th} = \frac{1}{w_{cw}/\rho_{cw} + w_{fs}/\rho_{fs}} \quad (3)$$

Total porosity was calculated according to Eq. (4), where  $P_t$  was the total porosity and  $\rho_{me}$  was the measured density of

samples.

$$P_t = \frac{\rho_{th} - \rho_{me}}{\rho_{th}} \quad (4)$$

The closed porosity  $P_c$  was calculated using Eq. (5), in which  $P_o$  was the measured open porosity.

$$P_c = P_t - P_o \quad (5)$$

As shown in Table 2, it could be concluded that the theoretical density increased linearly with the increasing content of FACs. Since the theoretical density of cenospheres wall was higher than that of silica, the theoretical density of composite ceramics with more cenospheres would be higher. However, in this experiment, the measured density decreased from 1.57 to 0.92 g/cm<sup>3</sup> as the content of FACs increased from 0 to 50 wt%. There were lots of hollow spaces in the FACs, which could lead to the closed pores forming in the composite samples. Therefore, as the number of FACs increased, the whole density of composite ceramics was lowered due to the formation of more closed pores.

The open porosity decreased with the increasing of FACs content. Fig. 4 shows the SEM images of S2 and S0 sintered at 1300 °C. The open porosities of S2 and S0 were 4% and 14%, separately. Apparently, S2 was sintered more densely than the pure silica ceramics. It demonstrated that FACs could promote the sintering property of silica ceramics. Shao [12] have reported that FACs improved the sintering property of Si<sub>3</sub>N<sub>4</sub> ceramics and the main chemical compositions of FACs, SiO<sub>2</sub> and Al<sub>2</sub>O<sub>3</sub> served as sintering aids. Furthermore, besides the composition of FACs, there was another reason for the densification of composite ceramics. In this experiment, when the temperature raised up to 1200 °C, part of the walls of fly ash cenospheres started to melt, which would promote the densification process of composite ceramics.

### 3.2. Effect of FACs on phase change

The XRD patterns of different samples were displayed in Fig. 5. The silica/FACs composite samples were composed of mullite, silicon oxide, quartz and glass phase after sintered at 1200 °C, and the cristobalite phase appeared when the composite samples were sintered at 1300 °C. However, in the pure silica ceramics, the cristobalite precipitated at 1200 °C. It indicated that some chemical composition in FACs could inhibit the crystallization of silica from amorphous phase to cristobalite phase.

Table 2  
The measured and calculated density of silica/FACs composites sintered at 1200 °C.

Weight percent of FACs/(%)	0	10	20	30	40	50
Theoretical density $\rho_{th}$ (g/cm <sup>3</sup> )	2.2	2.25	2.31	2.37	2.43	2.5
Measured density $\rho_{me}$ (g/cm <sup>3</sup> )	1.57	1.42	1.3	1.14	1.02	0.92
Total porosity $P_t$ (%)	29	37	44	51	58	63
Open porosity $P_o$ (%)	22	14	12	11	9	8
Closed porosity $P_c$ (%)	7	23	32	40	49	55
Specific surface area (m <sup>2</sup> /g)	–	69.32	80.55	92.00	100.68	106.52

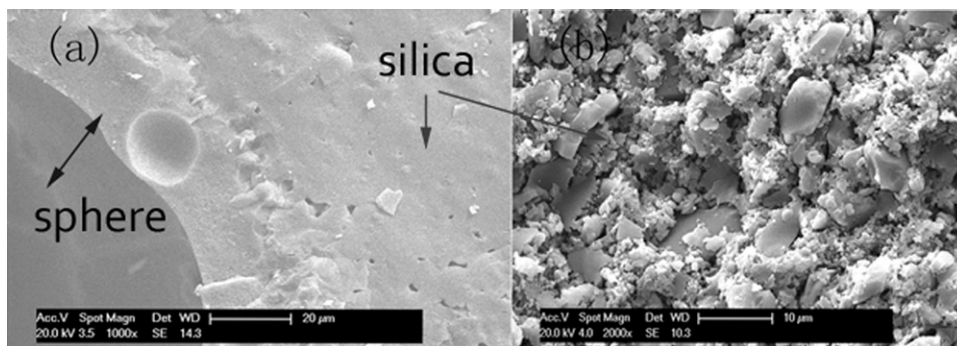


Fig. 4. SEM images of samples sintered at 1300 °C: (a) S2 sample and (b) S0 sample.

### 3.3. Microstructure

The microstructure of the sintered samples was shown in Fig. 6. The formation of uniform size of pores in the fracture section of S5 sintered at 1200 °C shown in Fig. 6(a) indicated that the porous silica-based composites were successfully prepared by using fly ash cenospheres as pore-forming agent. The magnified microstructure of Fig. 6(a) was shown in Fig. 6(b). Some lath-like mullites appeared on the boundary of two spheres. Fig. 6(c)–(f) shows the morphologies of S5 after leaching in 20 vol% HF for 10 min. As can be seen from the images, there were two kinds of mullites, lath-like and needle-like. The mullite (Fig. 6(c)) on the surface was lath-like, whose length may reach 20 μm (Fig. 6(f)), while the smaller and needle-like mullite appeared on the border of the spheres (Fig. 6(d)). It has been concluded by Dong [13] that for the low alumina content composite ceramics, the excessive liquid glass phase of low viscosity promoted the formation of whisker mullite crystals. It was apparently that the silica/FACs composites were low of alumina. In this paper, the forming of different morphologies of mullite whiskers may result from the different space sizes used for whiskers to grow. There were more free spaces on the surface of spheres than on the boundary.

As can be seen from Fig. 6(e) and (f), some lath-like mullites on the surface of the spheres were broken after leached in HF, indicating that there were part of mullites inserting into the silica matrix during sintering. As was reported [14],  $\text{Al}_2\text{O}_3$  is the main chemical composition in forming the mullite crystals and  $\text{Fe}_2\text{O}_3$  can promote the grain growth of mullite. In this experiment, there were  $\text{Al}_2\text{O}_3$  and  $\text{Fe}_2\text{O}_3$  in the FACs and  $\text{SiO}_2$  in the matrix. The diffusion of  $\text{Al}_2\text{O}_3$  and  $\text{Fe}_2\text{O}_3$  from FACs to the matrix during the sintering lead to the growth of the mullite. Plentiful lath-like mullite and needle-like mullite were interlaced with each other like a perfect 3-dimension fabric. The interlaced structure appeared on the discrete sphere and inserted into the matrix at the same time. The whole weave structure provided a powerful framework for the final products, which contributed a lot on the strength of composite ceramics.

### 3.4. Effect of FACs on the composites' strength

Flexural strength of silica/FACs composite samples sintered at different temperatures were shown in Fig. 7. The flexural strength firstly increased and then decreased as sintering temperature increased from 1100 to 1300 °C. Strength reached its highest value when the samples were sintered at 1200 °C. During the sintering process, the densification and cristobalite crystallization affected the flexural strength of samples obviously. The densification process dominated when the sintering temperature was from 1100 to 1200 °C. As a result, the flexural strength of samples increased with the sintering temperature. When the sintering temperature reached 1300 °C, the cristobalite crystallized and lowered the flexural strength of samples. As was proved in Fig. 5, there were plenty of cristobalite phase formed when the samples were sintered at 1300 °C. When the samples were cooled from high temperature to 170–270 °C, the high temperature  $\alpha$ -cristobalite would transform to the low temperature  $\beta$ -cristobalite, named displacive phase transition, and the fast phase transformation process lead to the formation of micro-cracks. The flexural strength deteriorated as a result.

The flexural strength and porosity of the samples as a function of FACs content were shown in Fig. 8. Comparing with the strength of samples without FACs, the strength of samples with 10 wt% FACs addition decreased dramatically. The strength increased subsequently as the content of FACs

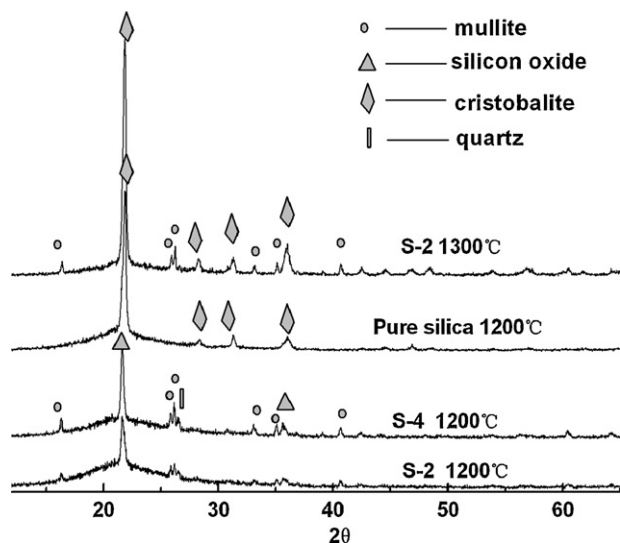


Fig. 5. XRD patterns of samples sintered at different temperatures.



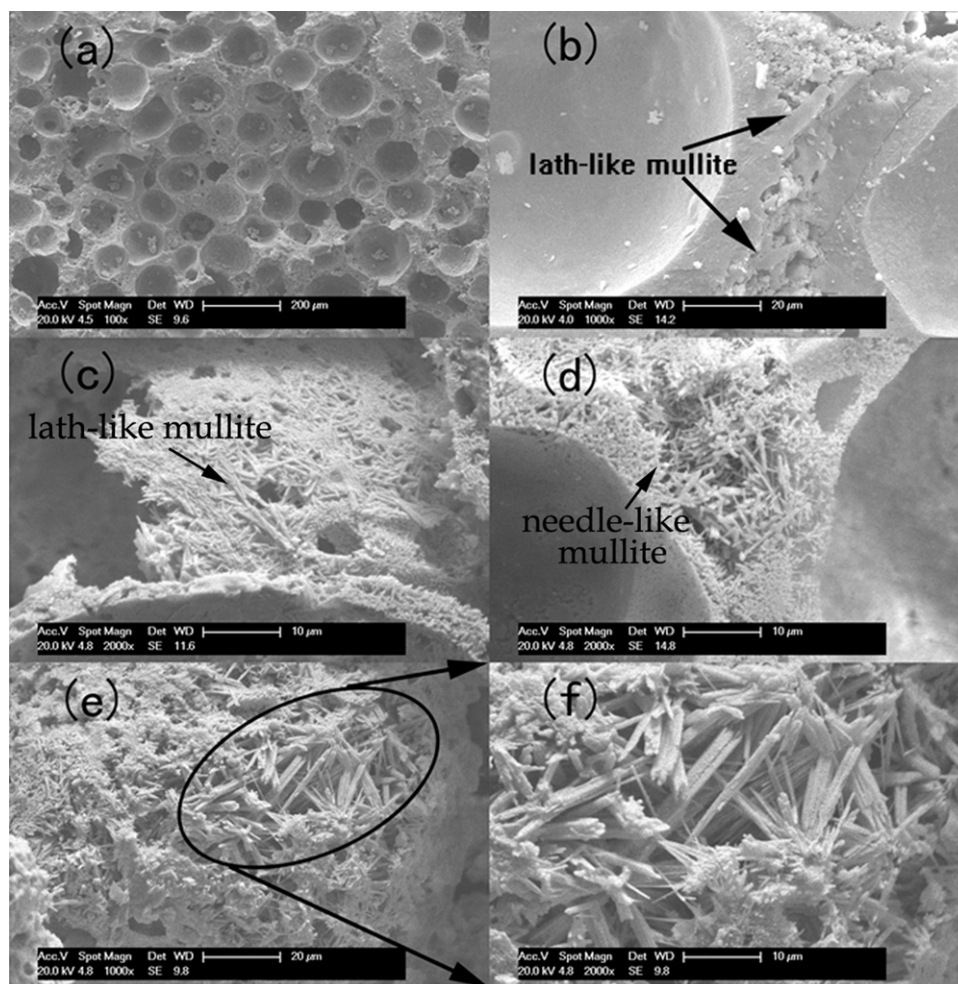


Fig. 6. SEM images of S5 samples sintered at 1200 °C: (a) and (b) were different magnification of samples and (c)–(f) were samples after treatment in HF.

increased from 10 to 50 wt%, although the porosity was higher. The reason was that the mullite crystals grew out from FACs to the matrix, which played an important role in strengthening. Though there were more pores when adding more FACs, the formation of mullite crystals could make the samples

strengthened. With the mullite framework, it was also easy to account for the phenomenon that the strength of samples S4 and S5 (porosity around 58–63%) was almost as high as that of the compact pure silica ceramic (around 13 MPa) when sintered at 1200 °C.

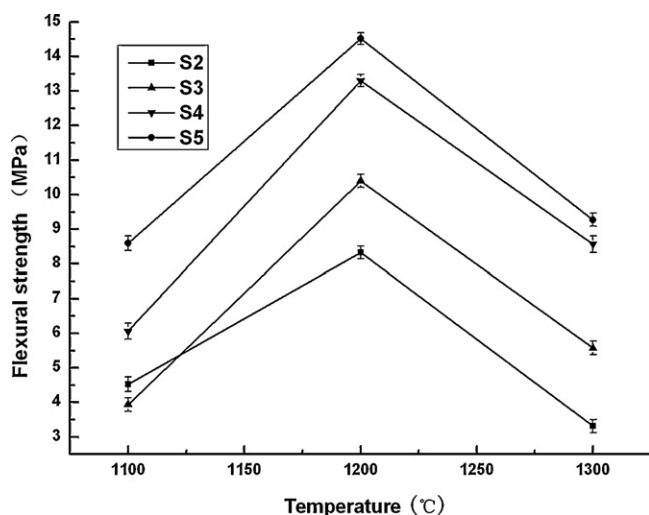


Fig. 7. Flexural strength of sintered samples.

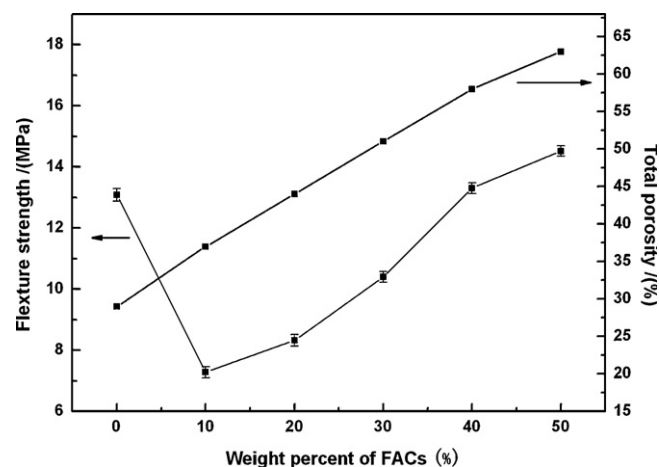


Fig. 8. Variations in flexural-strength and the porosity values versus FACs content.

#### 4. Conclusions

1. Silica-based composite, with the density of  $0.92 \text{ g/cm}^3$  and flexural strength of 14.5 MPa, were prepared by using fly ash cenospheres as density-decreasing agent and strengthening framework.
2. The density of the silica-based composites decreased as the content of fly ash cenospheres increased, while the strength increased inversely when the content of sphere was lower than 50 wt%.
3. In the process of sintering, FACs acted as a sintering aid to promote the densification of silica, and as an inhibitor to restrain the crystallization of cristobalite.
4. The growth of mullite from sphere to the matrix and the structure of 3-dimension mullite fabric provided a powerful framework for the final products.

#### Acknowledgements

This work was supported by the Natural Science Foundation of Tianjin under grant no. 08JCYBJC08800, and the National Natural Science Foundation of China under grant no. 50772073.

#### References

- [1] S.C. White, E.D. Case, Characterization of fly ash from coal-fired power plants, *J. Mater. Sci.* 25 (1990) 5215–5219.
- [2] P.K. Kolay, D.N. Singh, Physical, chemical, mineralogical and thermal properties of cenospheres from an ash lagoon, *Cem. Concr. Res.* 31 (2001) 539–542.
- [3] K.T. Varughese, B.K. Chaturvedi, Fly ash as fine aggregate in polyester based polymer concrete, *Cem. Concr. Compos.* 18 (1996) 105–108.
- [4] B. Yilmaz, A. Olgun, Studies on cement and mortar containing low-calcium fly ash, limestone, and dolomitic limestone, *Cem. Concr. Compos.* 30 (2008) 194–201.
- [5] D.P. Mondal, S. Das, N. Ramakrishnan, K.U. Bhasker, Cenosphere filled aluminum syntactic foam made through stir-casting technique, *Composites: Part A* 40 (2009) 279–288.
- [6] P.K. Rohatgi, J.K. Kim, N. Gupta, et al., Compressive characteristics of A356/fly ash cenosphere composites synthesized by pressure infiltration technique, *Composites: Part A* 37 (2006) 430–437.
- [7] N. Chand, P. Sharma, M. Fahim, Correlation of mechanical and tribological properties of organosilane modified cenosphere filled high density polyethylene, *Mater. Sci. Eng. A* 527 (2010) 5873–5878.
- [8] S.M. Kulkarni, Kishore, Studies on fly ash-filled epoxy-cast slabs under compression, *J. Appl. Polym. Sci.* 84 (2002) 2404–2410.
- [9] S.M. Kishore, D.S. Kulkarni, On the use of an instrumented set-up to characterize the impact behavior of an epoxy system containing varying fly ash content, *Polym. Test.* 21 (2002) 763–771.
- [10] Y.E. Pivinskii, F.T. Gorobets, High density fused silica ceramic, *Refract. Ind. Ceram.* 9 (2010) 509–516.
- [11] P.K. Rohatgi, A. Daoud, B.F. Schultz, T. Puri, Microstructure and mechanical behavior of die casting AZ91D-Fly ash cenosphere composites, *Composites: Part A* 40 (2009) 883–896.
- [12] Y.F. Shao, D.C. Jia, B.Y. Liu, Characterization of porous silicon nitride ceramics by pressureless sintering using fly ash cenosphere as a pore-forming agent, *J. Eur. Ceram. Soc.* 29 (2009) 1529–1534.
- [13] Y.C. Dong, J.D. Wu, X.F. Feng, et al., Phase evolution and sintering characteristics of porous mullite ceramics produced from the flyash- $\text{Al}(\text{OH})_3$  coating powders, *J. Alloys Compd.* 460 (2008) 651–657.
- [14] M. Ocaña, A. Caballero, C.T. González, C.J. Serna, Preparation by pyrolysis of aerosols and structural characterization of Fe-doped mullite powders, *Mater. Res. Bull.* 35 (2000) 775–788.